1-28-2015

Altered intrinsic functional coupling between core neurocognitive networks in Parkinson's disease

Deepti Putcha
Boston University

Robert S. Ross
The University of New Hampshire, robert.ross@unh.edu

Alice Cronin-Golomb
Boston University

Amy C. James
Harvard Medical School

Chantal E. Stern
Boston University

Recommended Citation

Deepti Putcha, Robert S. Ross, Alice Cronin-Golomb, Amy C. Janes, Chantal E. Stern, Altered intrinsic functional coupling between core neurocognitive networks in Parkinson's disease, NeuroImage: Clinical, Volume 7, 2015, Pages 449-455, ISSN 2213-1582, http://dx.doi.org/10.1016/j.nicl.2015.01.012.

NeuroImage: Clinical 7 (2015) 449–455

Contents lists available at ScienceDirect

NeuroImage: Clinical

journal homepage: www.elsevier.com/locate/ynicl

Altered intrinsic functional coupling between core neurocognitive networks in Parkinson's disease

Deepti Putcha[a,b,*], Robert S. Ross[a,b,c], Alice Cronin-Golomb[a], Amy C. Janes[d,1], Chantal E. Stern[a,b,1]

[a]Department of Psychological and Brain Sciences, Boston University, Boston, MA 02115, USA
[b]Athinoula A. Martinos Center for Biomedical Imaging, Massachusetts General Hospital, Boston, MA 02114, USA
[c]Department of Psychology, University of New Hampshire, Durham, NH 03824, USA
[d]McLean Imaging Center, McLean Hospital, Department of Psychiatry, Harvard Medical School, Belmont, MA 02478, USA

ARTICLE INFO

Article history:
Received 15 December 2014
Received in revised form 23 January 2015
Accepted 24 January 2015
Available online 28 January 2015

Keywords:
Parkinson's disease
fMRI
Functional connectivity
DMN
SN
CEN

ABSTRACT

Parkinson's disease (PD) is largely attributed to disruptions in the nigrostriatal dopamine system. These neurodegenerative changes may also have a more global effect on intrinsic brain organization at the cortical level. Functional brain connectivity between neurocognitive systems related to cognitive processing is critical for effective neural communication, and is disrupted across neurological disorders. Three core neurocognitive networks have been established as playing a critical role in the pathophysiology of many neurological disorders: the default-mode network (DMN), the salience network (SN), and the central executive network (CEN). In healthy adults, DMN–CEN interactions are anti-correlated while SN–CEN interactions are strongly positively correlated even at rest, when individuals are not engaging in any task. These intrinsic between-network interactions at rest are necessary for efficient suppression of the DMN and activation of the CEN during a range of cognitive tasks. To identify whether these network interactions are disrupted in individuals with PD, we used resting state functional magnetic resonance imaging (rsfMRI) to compare between-network connectivity between 24 PD participants and 20 age-matched controls (MC). In comparison to the MC, individuals with PD showed significantly less SN–CEN coupling and greater DMN–CEN coupling during rest. Disease severity, an index of striatal dysfunction, was related to reduced functional coupling between the striatum and SN. These results demonstrate that individuals with PD have a dysfunctional pattern of interaction between core neurocognitive networks compared to what is found in healthy individuals, and that interaction between the SN and the striatum is even more profoundly disrupted in those with greater disease severity.

1. Introduction

Many neurological and psychiatric disorders are associated with disrupted functional connectivity between important neurocognitive networks, providing insights into the aberrant brain organization inherent to these disorders. Large-scale network analysis exploring brain function across healthy adults and brain-disordered individuals has lead to a conceptual framework referred to as the triple network model of pathology. This model highlights three distributed neurocognitive networks which are critical to maintaining effective neural communication and are found to be disrupted across many neuropsychiatric disorders (Menon, 2011): the default-mode network (DMN), the salience network (SN), and the central executive network (CEN) (Greicius et al., 2003; Menon and Uddin, 2010; Seeley et al., 2007). Typically, the SN and CEN increase activation in response to external stimuli (Dosenbach et al., 2006), whereas DMN activity is suppressed, resulting in anti-correlated coupling between the CEN and DMN (Fox et al., 2005a; Greicius et al., 2003; Raichle et al., 2001). Interestingly, these same patterns of interaction among the three core neurocognitive networks are also observable in resting state fMRI data (Menon, 2011; Sridharan et al., 2008). Previous fMRI work demonstrates that resting brain organization is highly related to how the brain functions during external tasks (Fox et al., 2005a; van den Heuvel et al., 2009), suggesting that studying resting brain connectivity patterns will provide useful insight into neurobiology of disordered populations (Fox and Greicius, 2010; Raichle and Mintun, 2006; Shulman et al., 2004) including those with Parkinson's disease (PD).

In addition to the fact that interactions between these three core cognitive networks are disrupted across neuropsychiatric disorders, striatal dysfunction associated with PD (Ravina et al., 2012) may influence these network interactions. Through reciprocal connections,

* Corresponding Author: Center for Psychological and Brain Sciences, 2 Cummington Mall, Rm 109, Boston, MA 02215, USA. Tel: +1 617 353 1396.
E-mail address: dputcha@bu.edu (D. Putcha).
[1] Indicates co-last authorship.

http://dx.doi.org/10.1016/j.nicl.2015.01.012

striatal neurons are thought to coordinate activity in many cortical regions (Macdonald and Monchi, 2011), emphasizing the idea that PD pathology impacts widespread cortical regions as well as the basal ganglia. A recent resting state study in young adults found that the striatum interacts with regions comprising the DMN and SN (Di and Biswal, 2014). The striatum also is functionally and structurally connected with cortical areas that comprise the CEN through reciprocal circuitry with the dorsolateral prefrontal cortex and posterior parietal cortex (Alexander and Crutcher, 1990; Kish et al., 1988; Leh et al., 2008), which display abnormal activations in PD during cognitively demanding tasks (Carbon et al., 2010; Eidelberg, 2009; Lewis et al., 2003; Schendan et al., 2013; Tinaz et al., 2008). Decreased functional connectivity within the DMN has been observed in PD during the resting state (Tessitore et al., 2012) and during cognitively demanding tasks (van Eimeren et al., 2009), suggesting that disease-related network disruptions may influence the functional coupling between DMN–CEN interactions leading to heightened activation and dysfunctional connectivity of the DMN in PD. However, it remains to be elucidated if PD is associated with specific disruptions in functional coupling between the SN, CEN, and DMN.

Structurally, striatal neurons are highly interconnected with neurons in the insular cortex (Chikama et al., 1997; Fudge et al., 2005), an important node of the SN. Further, dopamine depletion is thought to occur in parallel in the striatum and the insula (Christopher et al., 2014b; Monchi et al., 2007; Shine et al., 2013). It has been hypothesized that the loss of D2 signaling in the insula disrupts the modulation of SN activity, impairing its function in coordinating interactions between other brain networks (Menon and Uddin, 2010). Altered cortico-striatal–thalamocortical neurocircuitry resulting from dysfunctional striatal dopaminergic function, as is observed in PD, is thought to lead to aberrant assignment of salience (Kish et al., 1988; Monchi et al., 2007; Shine et al., 2013), further emphasizing the association between the striatum and salience network in PD. As striatal dysfunction is characteristic of PD and worsens with disease severity, functional coupling between the striatum and the SN is also likely to be disrupted as a function of disease progression.

In the present study, we used resting state functional magnetic resonance imaging (rs-fMRI) to identify SN–DMN, SN–CEN and CEN–DMN interactions in a group of non-demented individuals with PD and age-matched healthy participants (MC). As disease severity in PD is correlated with increased striatal disruption (Lozza et al., 2002; Ravina et al., 2012), we also sought to determine whether disease severity was related to functional coupling between the striatum and the SN. We hypothesized that MC participants would demonstrate negative DMN coupling with SN and CEN, and positive SN coupling with CEN, consistent with the observed patterns in young neurologically normal adults (Fox et al., 2005a; Sridharan et al., 2008). In contrast, we expected dysfunctional SN coupling with the DMN and CEN in PD participants compared to MC. We also predicted that within the group of PD individuals, increased disease severity would be related to reduced SN–striatum functional coupling.

2. Methods

2.1. Participants

Twenty-six individuals diagnosed with PD and 24 healthy MC adults were enrolled. Two individuals with PD and 4 MC participants were excluded on the basis of excess motion (greater than 2 mm displacement) in the magnetic resonance imaging (MRI) scanner, resulting in a total of 24 PD (12 female, mean age 62.5 years, 2 left-handed) and 20 MC (11 female, mean age 65.9 years, 2 left-handed) participants (Table 1). All participants provided informed consent in a manner approved by the institutional review boards of Boston University and Partners Human Research Committee. All participants were screened for other neurological and psychiatric illness via self-report questionnaires and physician record confirmation.

Table 1
Participant characteristics.

	PD (N = 24)	MC (N = 20)
Age (years)	62.5 ± 6.4	65.9 ± 9.4
Male/female	12/12	9/11
Education (years)	17.6 ± 2.2	16.6 ± 2.2
MMSE (out of 30)	28.6 ± 0.9	28.8 ± 0.8
BDI-II	5.8 ± 4.4*	2.3 ± 2.9
BAI	5.3 ± 3.7**	1.5 ± 2.1
UPDRS total	27.1 ± 10.8	–
UPDRS motor	16.1 ± 7.2	–
Levodopa equivalent dosage (mg/day)	368.9 ± 261.9	–
Hoehn and Yahr	2 (median); 1 (min) to 3 (max)	–
RPD/LPD	13/11	–
T-PD/AR-PD/G-PD	12/7/5	–

MMSE: Mini-Mental State Examination. UPDRS: Unified Parkinson's Disease Rating Scale. BDI-II: Beck Depression Inventory, 2nd Edition. BAI: Beck Anxiety Inventory. RPD: Right-side of body symptom at onset. LPD: Left-side of body symptom at onset. T-PD: Tremor at onset. AR-PD: Akinetic–Rigid at onset. G-PD: Gait-instability at onset.
Values presented in the table are means ± standard deviations, unless otherwise noted.
* Indicates group differences at a significance level of $p < 0.05$.
** Indicates group differences at a significance level of $p < 0.005$.

Participants diagnosed with idiopathic PD were recruited from the Parkinson's Disease Center at Boston Medical Center. All participants taking anti-parkinsonian medications were scanned at peak "ON" levels of medication, approximately 60–90 min after the optimized daily dose was taken. All of the participants with PD were on a combination of levodopa–carbidopa, dopamine receptor agonists, or monoamine oxidase B inhibitors. Three were also on antidepressant medication, and two of those three were also taking anti-anxiety medication as needed. All participants completed self-report mood inventories including the Beck Depression Inventory (BDI-II) and the Beck Anxiety Inventory (BAI); control participants reported minimal symptoms of anxiety and depression while PD participants reported very mild levels of anxiety and depression (Table 1). While there are statistical differences between PD and MC groups on anxiety and depression scores, all participants were well below clinically significant levels of anxiety and depression disorder. No participant reported major mood or behavioral disturbance. Levodopa equivalent dosage (LED) was calculated as per recent convention (Tomlinson et al., 2010) to be 368.9 mg/day on average in the PD group. All PD participants met the clinical criteria for mild to moderate disease staging (Hoehn and Yahr stages I-III) as assessed by the Unified Parkinson's Disease Rating Scale (UPDRS) (MDS, 2003). The median Hoehn and Yahr staging was 2, ranging from 1 (unilateral) to 3 (moderate bilateral). Out of 24 participants with Parkinson's disease, 3 patients were classified as Hoehn and Yahr stage 1, 4 participants as stage 1.5, 12 participants as stage 2, 3 participants as stage 2.5, and 2 participants as stage 3. Twelve participants identified tremor as being their initial symptom, 7 participants identified rigidity, and 5 participants identified difficulty with gait or balance. Average total score on the UPDRS was 27.1 and average motor subscore was 16.1 (Table 1). Average disease duration of the PD group overall was 5.6 years. The average disease duration of PD individuals whose initial symptom was tremor was 5.9 years and for those whose initial symptom was akinetic/rigid was 5.3 years, which was not significantly different ($p > 0.5$). Of the 24 PD participants, 13 were classified as right-onset (RPD) and 11 were classified as left-onset (LPD). Average disease duration of LPD participants was 4.5 years, and average disease duration of RPD participants was 6.5 years, which was not statistically different ($p > 0.2$).

All participants were screened for contraindications to MRI. At study entry, the modified Mini-Mental State Examination (MMSE) was administered to screen for mental status. These scores were converted to standard MMSE scores on a scale of 30; all participants were classified as non-demented, averaging 28 points out of 30 (Table 1). Although

the MMSE score by itself is not sufficient to rule out any cognitive impairment, the objective of this cognitive screen was to ensure that all participants were above the generally accepted criteria for dementia, which is below 24 points out of 30 (Dick et al., 1984). All participants received detailed health history screening and a neuro-ophthalmological examination to ensure eye integrity and rule out ocular disease or abnormality. A normal anatomical brain without any evidence of gross abnormalities (i.e. infarct, tumor) was necessary for study inclusion. Other exclusionary criteria included coexisting, chronic medical illnesses, use of psychoactive medication besides antidepressants and anxiolytics in the MC group (allowed in PD), history of intracranial surgery or head trauma resulting in a loss of consciousness, and history of drug and alcohol abuse.

2.2. Neuroimaging procedure

Each scanning session included 20 min of structural imaging sequences followed by resting state data acquisition lasting 6 min and 35 s, during which the participants were asked to remain still and maintain eyes-open fixation on a projected image of a white cross on a black background. All scanning was performed using a 12-channel head coil in a Siemens Trio 3 T scanner (Siemens Medical Systems, Erlangen, Germany) at the Athinoula A. Martinos Center for Biomedical Imaging at Massachusetts General Hospital. T_1-weighted Magnetization Prepared-Rapid Acquisition Gradient Echo (MP-RAGE) structural scans were acquired using generalized auto-calibrating partially parallel acquisition (GRAPPA): repetition time = 2530 ms, echo time = 3.44 ms, inversion time = 1100 ms, flip angle = 7 degrees, field of view = 256 mm, slice thickness = 1 mm, 176 sagittal slices (right to left). The functional blood oxygen level dependent (BOLD) resting state fMRI data were acquired using a T_2^*-weighted gradient-echo echo-planar imaging (EPI) sequence: TR = 5000 ms, TE = 30 ms, FA = 90 degrees, FOV = 256 mm, in-plane resolution 4×4 mm^2. Fifty-five axial (anterior to posterior) slices with a thickness of 2 mm were acquired, oriented parallel to the anterior–posterior commissural line 76 whole-brain acquisitions were collected, and the first 5 acquisitions were subsequently discarded during image processing as "dummy" TRs for T_1 stabilization, resulting in 71 acquisitions being analyzed.

2.3. Image processing

Data pre-processing included: motion correction with MCFLIRT (Jenkinson et al., 2002), brain extraction using BET (Smith, 2002), spatial smoothing with a Gaussian kernel of full-width half-maximum 6 mm, and high-pass temporal filter with Gaussian-weighted least-squares straight-line fitting with $\sigma = 100$ s. Registration of the functional EPI volumes to each individual subject's high-resolution MPRAGE image and registration of MPRAGE to the MNI 152 2 mm^3 standard space template (Montreal Neurological Institute, Montreal, QC, Canada) were both accomplished using FLIRT. Four-dimensional time series data for all participants were transformed into standard space at 2 mm isotropic resolution using the registration transformation matrices.

2.4. ICA-based denoising

After ensuring no group differences in motion during scanning ($p > 0.7$, MC absolute mean displacement was 0.33 ± 0.19 mm; PD absolute mean displacement was 0.35 ± 0.19 mm), we conducted an ICA-based denoising approach to remove independent components within each individual subject's data that represented noise, including motion and scanner artifact. Independent components analysis (ICA) at the single subject level was conducted using the FSL program MELODIC (Jenkinson et al., 2012; McKeown et al., 2003). For every participant, all components were visually inspected (Kelly et al., 2010), and all identified sources of noise were removed using FSL's *fsl_regfilt* utility.

2.5. Inter-network functional coupling

The default mode (DMN), central executive (CEN), and salience networks (SN) were defined using a previously published set of templates from the BrainMap Database (Fig. 1) (Fox et al., 2005b; Laird et al., 2005; Laird et al., 2011). FSL's dual regression approach was used to calculate the subject specific orthogonal timecourses and spatial maps for each network of interest (Beckmann et al., 2009; Cole et al., 2010; Filippini et al., 2009; Janes et al., 2012, 2014). Subject-specific timecourses were extracted from the SN, DMN, R- and L-CEN. The CEN in this study was defined as right- and left-hemisphere localized networks, as it was in the BrainMap database template (Fig. 1). Correlation coefficients (Pearson's r) were computed between the SN and DMN, the SN and CEN (both right and left hemispheres), and between the CEN (both right and left hemispheres) and DMN. Pearson's r coefficients were computed for each individual in first level analysis, and later used for second-level group comparison analysis. Though some of these networks include overlapping brain regions (i.e. posterior parietal lobe), this dual regression approach identifies orthogonal timecourses that are used in subsequent analysis. Independent samples *t-tests* were conducted to compare MC and PD participants on coupling values between the SN and DMN, the SN and CEN, and between the DMN and CEN. To investigate if PD disease duration or dopamine replacement medication were related to these inter-network functional coupling measures, correlation coefficients (Pearson's r) were computed between disease duration (number of years), levodopa equivalent dosage, and the functional coupling values described above.

2.6. Striatal–salience network interactions

FreeSurfer automated structural parcellations were used to define each individual's entire putamen and caudate volume labels, which were combined to create a "striatum" region of interest (ROI) specific to each individual. It should be noted that while the ventral components of the caudate and putamen were included in our striatal ROI, the nucleus accumbens was not. Thus, our striatal ROI focuses on the dorsal striatum. Timecourses from each participant's striatal ROI were extracted and correlated with the salience network timecourse. To determine the relationship between striatal coupling with the salience network and PD symptom severity, we correlated this coupling measure with the UPDRS total score.

2.7. Volumetric analysis

To ensure that volumetric differences between MC and PD participants were not impacting our results, the following analyses were conducted. MP-RAGE images were processed using FreeSurfer (version 5.3.0) (http://surfer.nmr.mgh.harvard.edu). Standard preprocessing of structural volumes produced reconstructions that were used to determine if there were any areas of cortical thinning or subcortical atrophy in the PD group compared to MC using the QDEC utility. We also compared striatal volume between MC and PD groups to determine if there were any volumetric differences in the seed region.

3. Results

3.1. No group differences in age, education, male-to-female ratio, mental status, cortical thinning or brain volume

MC and PD participants were matched on age ($p > 0.2$), education ($p > 0.1$), male-to-female ratio ($\chi^2 = 0.11$, $p > 0.7$), and MMSE scores ($p > 0.5$, range 25.7–29.7). There were no between-group differences in whole brain cortical thinning or subcortical atrophy ($p > 0.05$,

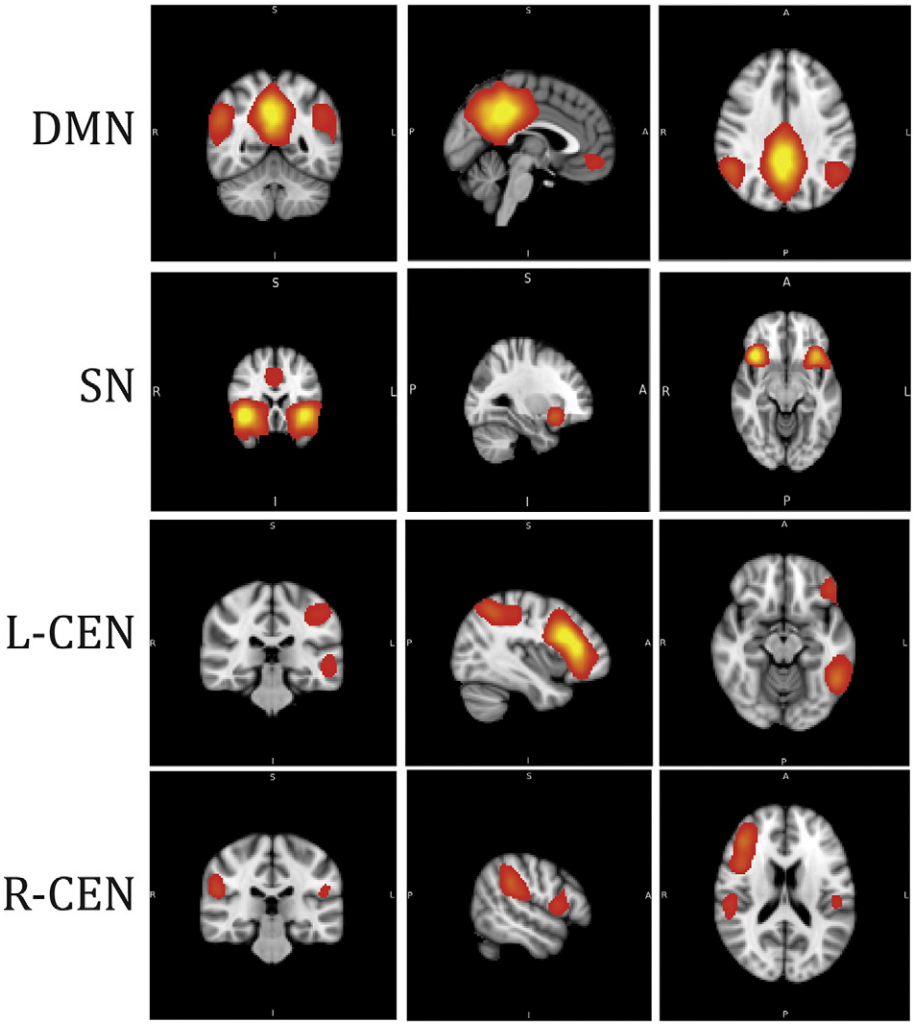

Fig. 1. Three core neurocognitive networks include the default mode network (DMN), salience network (SN), and central executive network separated by left- and right-hemisphere localization (L-CEN and R-CEN). Images are from a previously published set of templates from the BrainMap Database (Laird et al., 2005).

Bonferroni corrected), and no group differences in striatal volume after controlling for intracranial volume ($p > 0.4$).

3.2. Inter-network functional coupling disrupted in PD

We observed significant group differences in functional coupling between the SN and R-CEN ($t = 2.4$, $p = 0.02$, Fig. 2a), and between the DMN and R-CEN ($t = -2.1$, $p = 0.04$, Fig. 2b). Specifically, SN coupling with R-CEN was significantly more positive in MC compared to PD. In examining inter-network coupling of DMN with R-CEN, MC demonstrated negative coupling whereas PD demonstrated positive coupling between these networks. We did not observe differences in functional coupling between the L-CEN and either the DMN ($t = 0.35$, $p = 0.73$) or SN ($t = -1.05$, $p = 0.31$). We observed no significant associations between levodopa equivalent dosage (LED) and these measures of functional coupling (all $p > 0.46$), suggesting that dopamine replacement

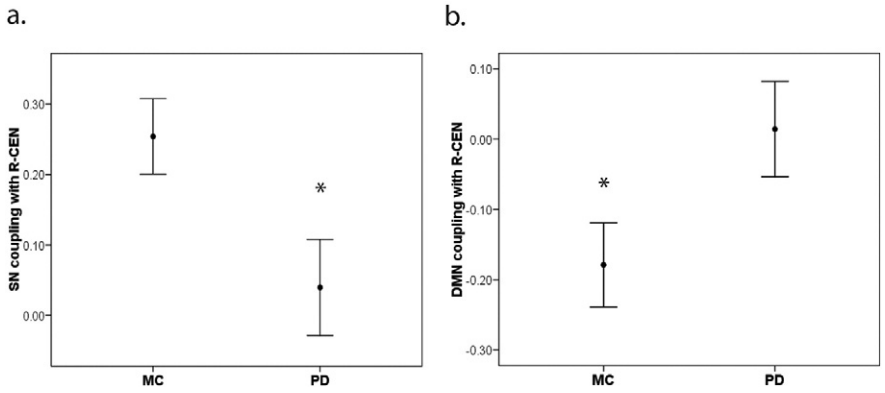

Fig. 2. In MC compared to PD, we observed (a) more positive SN coupling with R-CEN ($t = 2.4$, df = 42, $p = 0.02$), and (b) more negative DMN coupling with R-CEN ($t = -2.1$, df = 42, $p = 0.04$).

therapy is not likely to be the explanation of our findings of disrupted inter-network coupling in PD.

3.3. SN–striatal functional coupling decreased in relation to disease severity

Striatal coupling with the salience network was related to disease severity as measured by the UPDRS total score ($r = -0.45$, $p = 0.03$) such that more severe disease was associated with diminished functional coupling between the SN and striatum (Fig. 3). For many of these individuals, more severe disease was associated with reduced positive functional coupling between the striatum and SN, but those individuals with the most severe disease demonstrated anti-correlation in the functional coupling between the SN and striatum. A UPDRS motor sub-score, specifically focusing on severity of the cardinal motor symptoms of PD, was also associated with diminished SN–striatum functional coupling at the level of a trend ($r = -0.40$, $p = 0.06$). Interestingly, SN–striatum functional coupling was significantly related to functional coupling between the SN and CEN (hemisphere averaged) in the PD group ($F = 0.53$, $p = 0.031$) but not in the MC group ($F = 0.98$, $p = 0.03$). We observed no significant association between SN–striatum coupling and LED ($r = -0.11$, $p = 0.6$), suggesting that dopamine replacement is not likely to be related to disrupted SN–striatum coupling. We did not observe statistical differences in the association between disease severity and SN–striatum coupling between LPD and RPD subtypes ($p > 0.2$).

4. Discussion

We identified disruptions in resting state functional connectivity between large-scale core neurocognitive networks in PD. Specifically, individuals with PD showed connectivity patterns in opposition to what is reported in healthy individuals (Fox et al., 2005a; Menon, 2011; Sridharan et al., 2008). We observed an aberrant positive coupling between the R-CEN and DMN in PD, compared to the expected anti-correlation we observed between these two networks in the healthy control group. We also found a reduction in coupling strength between the SN and R-CEN in PD compared to healthy matched adults. The triple network model (Menon, 2011) posits that positive SN–CEN interactions and negative CEN–DMN interactions at rest allow for successful recruitment of the CEN and suppression of the DMN during cognitively challenging task demands. This connectivity among the salience, central executive, and default mode neurocognitive networks is very important to promote efficient cognitive processing in a healthy individual and becomes dysfunctional across a number of brain disorders (Menon, 2011; Seeley et al., 2007). This study demonstrates disrupted intrinsic network interactions among these three neurocognitive networks in PD, providing evidence of disruptions to cortical organization and connectivity in this disease.

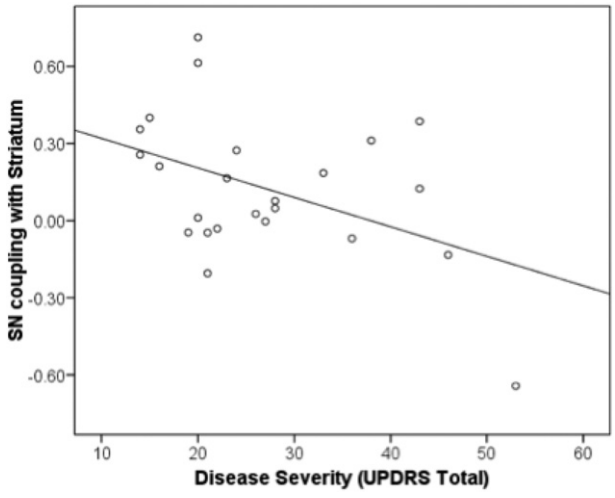

Fig. 3. Disease severity as measured by the Unified Parkinson's Disease Rating Scale was correlated with functional coupling between the striatum and salience network (SN; $r = -0.45$, $p = 0.03$), such that less positive coupling of these networks was associated with worse disease severity. Each point on the plot represents an individual with PD.

In the healthy brain, the SN and CEN are positively coupled, while the DMN and CEN are anti-correlated (Fox et al., 2005a; Menon, 2011; Sridharan et al., 2008). The inter-network interactions we observed in our healthy age-matched control population are consistent with these findings in young adults. By contrast, the PD group demonstrated an altered pattern of network interactions. Specifically, in PD we observed *positive* coupling between the R-CEN and DMN, compared to the anti-correlation seen in younger adults (Fox et al., 2005a; Sridharan et al., 2008) and our healthy older control participants, possibly reflecting a failure to suppress DMN activity (van Eimeren et al., 2009) or a failure of modulating top-down signals between the DMN and CEN, as has been previously suggested (Anticevic et al., 2012). This pattern of dysfunctional DMN large-scale network connectivity is also present in other dopaminergic disorders, such as schizophrenia (Ongur et al., 2010), as well as in other neurodegenerative disorders including Alzheimer's disease (Greicius et al., 2004; Supekar et al., 2008).

We also observed reduced functional coupling between the SN and R-CEN in PD compared to the control participants. The insula and dorsal anterior cingulate cortex, key nodes of the salience network (Seeley et al., 2007), are anatomically connected and functionally co-activated with the CEN (Menon and Uddin, 2010; Seeley et al., 2007). PD pathology proceeds from the striatum to widespread cortical regions, including the insular cortex, soon after manifestation of motor symptomatology (Christopher et al., 2014b; Disbrow et al., 2014; Kish et al., 1988). Specifically, evidence of alpha-synuclein deposition, a key feature of PD pathology, is detected in the insula by Braak stage 3 (Braak et al., 2006b), when clinical motor signs of parkinsonism become apparent (Burke et al., 2008). In the current project, a trend level association was found between the UPDRS motor score and striatal–SN functional coupling, suggesting that disruptions to these networks are relevant to specific motor symptom manifestations of PD. By Braak stage 5, these pathological changes appear to cause alterations of dopamine receptor function and synaptic activity in the insula, contributing to cognitive and autonomic symptoms in PD (Braak et al., 2006a; Christopher et al., 2014a). These pathological changes in the insula likely impact the ability of the SN to effectively recruit and communicate with other neocortical regions such as the dorsolateral prefrontal cortex and posterior parietal cortices that comprise the CEN (Christopher et al., 2014b; Sridharan et al., 2008). The changes we observed in SN–CEN network coupling may reflect increased PD-related pathological burden in the striatum and insula, as is supported by our finding of striatal–SN coupling being significantly related to SN–CEN coupling in PD but not in MC.

Increased PD pathology and dopamine deficiency have been observed as occurring in parallel in the striatum and insula. Recent work has shown that PD patients diagnosed with mild cognitive impairment differed from cognitively normal PD by the presence of greater striatal dopamine depletion related to more D2 receptor loss in the insula (Christopher et al., 2014b). We observed a breakdown of intrinsic functional coupling between the SN and striatum related to increased disease severity. This observation suggests that PD-related striatal dysfunction may lead to functional disruptions in the communication between the striatum and the insula. We postulate that increased pathology in these regions and further breakdown in communication between them likely continues as PD progresses, contributing to the worsening of cognitive and autonomic symptoms observed in later stages of the disease. Understanding the association between breakdown in functional coupling between these core neurocognitive networks and cognitive performance will be an important focus of future study.

We observed disruptions specific to the right-hemisphere localized central executive network (R-CEN). One possible explanation could be that the L-CEN is localized entirely to the left hemisphere and is implicated strongly with language, verbal memory, and working memory (Laird et al., 2011). In contrast, the R-CEN reaches across both hemispheres in the parietal lobe and is thought to be involved in more widespread cognitive functions including reasoning, attention, inhibition, and memory (Laird et al., 2011). A recent study in healthy young adults of hemispheric localization within the CEN and coupling to other networks during the resting state suggests that the left-hemisphere localized CEN is strongly coupled with the DMN and language-related regions in the left-hemisphere, while the right-hemisphere localized CEN is preferentially coupled to the insula and regions of the brain specialized for attention processing (Wang et al., 2014). This asymmetric specialization of the CEN at rest and stronger preference of DMN to be functionally coupled with L-CEN than R-CEN may set the stage for vulnerability in R-CEN coupling with the DMN in older adults and individuals with neurological disease. Further, preferential coupling between the R-CEN and insula (Wang et al., 2014) combined with previously described vulnerability of the insula and attention networks in PD (Christopher et al., 2014a) could further explain why we see aberrant functional coupling specific to the R-CEN but not L-CEN. We do not ascribe this difference in network coupling in the CEN to lateralization of symptoms, as there were no significant subgroup differences in functional coupling with the CEN between RPD and LPD participants. However, these findings of lateralization could also be incidental. Future work examining PD performance across a more extensive neuropsychological assessment battery and with a larger sample size is needed in order to confirm the lateralization of network level findings in the CEN.

There is some evidence from previously published literature that dopaminergic therapy diminishes DMN integrity (Krajcovicova et al., 2012) and is differentially linked to spatial remapping of corticostriatal connectivity in chronically medicated and drug-naïve patients, such that drug-naïve patients demonstrated striatal hyperconnectivity with cortical regions and PD individuals ON medication demonstrated a general decrease in connectivity strength (Kwak et al., 2010). In the current study, PD participants were evaluated only on peak levels of dopaminergic medications, which limits our ability to address questions related to the effects of dopamine on neurocognitive network interactions. Although our approximation of levodopa equivalent dosage (LED) is not correlated significantly with SN–striatum coupling, we cannot with certainty rule out the possibility that dopamine medication is related in some way to the lower levels of functional coupling we observed between SN and striatum. Despite this limitation, it is worth noting that we did not detect any significant association between any of our functional coupling results and levodopa equivalent dosage (LED). Examining the network connectivity of PD individuals on medication has great utility because most patients experience cognitive dysfunction and disrupted activities in daily living even during peak medication states. Previous work has also shown that dopamine replacement therapy does not ameliorate cognitive disturbances in attentional set-shifting and other aspects of executive functioning (Lewis et al., 2005; Poletti and Bonuccelli, 2013), supported by the neurocognitive networks examined in our study.

We provide evidence in this study of disruptions in the functional coupling among three core neurocognitive networks in participants with PD. Typically, the SN interacts causally with the CEN and the DMN in that increased SN activity correlates with increased activity in the CEN and decreased activity in the DMN. This pattern of interactions is observed both during cognitive tasks and the resting state (Menon, 2011; Seeley et al., 2007; Sridharan et al., 2008), reflecting an intrinsic shifting of attention between external and internal processes. Functional activity in the SN and CEN typically increases during cognitive tasks in response to external stimuli (Dosenbach et al., 2006), whereas DMN activity is suppressed during externally-guided cognitive tasks (Greicius et al., 2003; Raichle et al., 2001), resulting in anti-correlations between the CEN and DMN. Our findings demonstrate aberrant positive CEN coupling with DMN and reduced SN coupling with CEN in PD. Further, our results demonstrate that functional coupling between the striatum and the SN is diminished as disease severity increases. The observed changes in intrinsic functional coupling discussed in this study represent an overarching framework for understanding cortical disruption in PD, similar to the cortical disruption that takes place in the context of other neurodegenerative diseases (Menon, 2011).

Conflicts of interest

The authors declare no competing financial interests.

Source of funding

This work was supported by the National Institute of Health R01 NS067128. Scanning was carried out at the Athinoula A. Martinos Center for Biomedical Imaging at the Massachusetts General Hospital, which receives funding from P41EB015896, a Biotechnology Resource Grant supported by the National Institute of Biomedical Imaging and Bioengineering (NIBIB), National Institutes of Health. This work also involved the use of instrumentation supported by the NIH Shared Instrumentation Grant Program and/or High-End Instrumentation Grant Program; specifically, grant number(s) S10RR022976 and S10RR019933. We also acknowledge salary funding for ACJ from grant number K01DA029645.

References

Alexander, G.E., Crutcher, M.D., 1990. Functional architecture of basal ganglia circuits: neural substrates of parallel processing. Trends Neurosci. 13 (7), 266–271. http://dx.doi.org/10.1016/0166-2236(90)90107-L1695401.

Anticevic, A., Cole, M.W., Murray, J.D., Corlett, P.R., Wang, X.J., Krystal, J.H., 2012. The role of default network deactivation in cognition and disease. Trends Cogn. Sci. 16 (12), 584–592. http://dx.doi.org/10.1016/j.tics.2012.10.00823142417.

Beckmann, C.F., Mackay, C.E., Filippini, N., Smith, S.M., 2009. Group comparison of resting-state FMRI data using multi-subject ICA and dual regression. NeuroImage 47, S148. http://dx.doi.org/10.1016/s1053-8119(09)71511-3.

Braak, H., Bohl, J.R., Müller, C.M., Rüb, U., de Vos, R.A.I., Del Tredici, K., 2006a. Stanley Fahn lecture 2005: the staging procedure for the inclusion body pathology associated with sporadic Parkinson's disease reconsidered. Mov. Disord. 21 (12), 2042–2051. http://dx.doi.org/10.1002/mds.21065.

Braak, H., Rüb, U., Schultz, C., Del Tredici, K., 2006b. Vulnerability of cortical neurons to Alzheimer's and Parkinson's diseases. J. Alzheimers Dis. 9 (3 Suppl), 35–4416914843.

Burke, R.E., Dauer, W.T., Vonsattel, J.P., 2008. A critical evaluation of the Braak staging scheme for Parkinson's disease. Ann. Neurol. 64 (5), 485–491. http://dx.doi.org/10.1002/ana.2154119067353.

Carbon, M., Reetz, K., Ghilardi, M.F., Dhawan, V., Eidelberg, D., 2010. Early Parkinson's disease: longitudinal changes in brain activity during sequence learning. Neurobiol. Dis. 37 (2), 455–460. http://dx.doi.org/10.1016/j.nbd.2009.10.02519900556.

Chikama, M., McFarland, N.R., Amaral, D.G., Haber, S.N., 1997. Insular cortical projections to functional regions of the striatum correlate with cortical cytoarchitectonic organization in the primate. J. Neurosci. 17 (24), 9686–97059391023.

Christopher, L., Koshimori, Y., Lang, A.E., Criaud, M., Strafella, A.P., 2014a. Uncovering the role of the insula in non-motor symptoms of Parkinson's disease. Brain 137 (8), 2143–2154. http://dx.doi.org/10.1093/brain/awu08424736308.

Christopher, L., Marras, C., Duff-Canning, S., Koshimori, Y., Chen, R., Boileau, I., Segura, B., Monchi, O., Lang, A.E., Rusjan, P., Houle, S., Strafella, A.P., 2014b. Combined insular and striatal dopamine dysfunction are associated with executive deficits in Parkinson's disease with mild cognitive impairment. Brain 137 (2), 565–575. http://dx.doi.org/10.1093/brain/awt33724334314.

Cole, D.M., Beckmann, C.F., Long, C.J., Matthews, P.M., Durcan, M.J., et al., 2010. Nicotine replacement in abstinent smokers improves cognitive withdrawal symptoms with modulation of resting brain network dynamics. NeuroImage 52, 590–599. http://dx.doi.org/10.1016/j.neuroimage.2010.04.251.

Di, X., Biswal, B.B., 2014. Modulatory interactions between the default mode network and task positive networks in resting-state. PeerJ 2, e367. http://dx.doi.org/10.7717/peerj.36724860698.

Dick, J.P., Guiloff, R.J., Stewart, A., Blackstock, J., Bielawska, C., Paul, E.A., Marsden, C.D., 1984. Mini-mental state examination in neurological patients. J. Neurol. Neurosurg. Psychiatry 47 (5), 496–499. http://dx.doi.org/10.1136/jnnp.47.5.4966736981.

Disbrow, E.A., Carmichael, O., He, J., Lanni, K.E., Dressler, E.M., Zhang, L., Malhado-Chang, N., Sigvardt, K.A., 2014. Resting state functional connectivity is associated with cognitive dysfunction in non-demented people with Parkinson's disease. J. Parkinsons Dis. 4 (3), 453–465. http://dx.doi.org/10.3233/JPD-13034124662193.

Dosenbach, N.U., Visscher, K.M., Palmer, E.D., Miezin, F.M., Wenger, K.K., Kang, H.C., Burgund, E.D., Grimes, A.L., Schlaggar, B.L., Petersen, S.E., 2006. A core system for

the implementation of task sets. Neuron 50 (5), 799–812. http://dx.doi.org/10.1016/j.neuron.2006.04.03116731517.
Eidelberg, D., 2009. Metabolic brain networks in neurodegenerative disorders: a functional imaging approach. Trends Neurosci. 32 (10), 548–557. http://dx.doi.org/10.1016/j.tins.2009.06.00319765835.
Filippini, N., MacIntosh, B.J., Hough, M.G., Goodwin, G.M., Frisoni, G.B., et al., 2009. Distinct patterns of brain activity in young carries of the APOE-epsilon4 allele. Proc. Natl. Acad. Sci. USA 106, 7209–7214. http://dx.doi.org/10.1073/pnas.0811879106.
Fox, M.D., Greicius, M., 2010. Clinical applications of resting state functional connectivity. Front. Syst. Neurosci. 4, 19. http://dx.doi.org/10.3389/fnsys.2010.0001920592951.
Fox, M.D., Snyder, A.Z., Vincent, J.L., Corbetta, M., Van Essen, D.C., Raichle, M.E., 2005a. The human brain is intrinsically organized into dynamic, anticorrelated functional networks. Proc. Natl. Acad. Sci. U S A 102 (27), 9673–9678. http://dx.doi.org/10.1073/pnas.050413610215976020.
Fox, P.T., Laird, A.R., Fox, S.P., Fox, P.M., Uecker, A.M., Crank, M., Koenig, S.F., Lancaster, J.L., 2005b. BrainMap taxonomy of experimental design: description and evaluation. Hum. Brain Mapp. 25 (1), 185–198. http://dx.doi.org/10.1002/hbm.2014115846810.
Fudge, J.L., Breitbart, M.A., Danish, M., Pannoni, V., 2005. Insular and gustatory inputs to the caudal ventral striatum in primates. J. Comp. Neurol. 490 (2), 101–118. http://dx.doi.org/10.1002/cne.2066016052493.
Greicius, M.D., Krasnow, B., Reiss, A.L., Menon, V., 2003. Functional connectivity in the resting brain: a network analysis of the default mode hypothesis. Proc. Natl. Acad. Sci. U S A 100 (1), 253–258. http://dx.doi.org/10.1073/pnas.013505810012506194.
Greicius, M.D., Srivastava, G., Reiss, A.L., Menon, V., 2004. Default-mode network activity distinguishes Alzheimer's disease from healthy aging: evidence from functional MRI. Proc. Natl. Acad. Sci. U S A 101 (13), 4637–4642. http://dx.doi.org/10.1073/pnas.030862710115070770.
Janes, A.C., Nickerson, L., Frederick, B.B., Kaufman, M.J., 2012. Prefrontal and limbic resting state brain network functional connectivity differs between nicotine-dependent smokers and non-smoking controls. Drug Alcohol Depend. 125, 252–259.
Janes, A.C., Farmer, S., Frederick, B.B., Nickerson, L.D., Lukas, S.E., 2014. An increase in tobacco craving is associated with enhanced medial prefrontal cortex network coupling. Plos One e88228.
Jenkinson, M., Bannister, P., Brady, M., Smith, S., 2002. Improved optimization for the robust and accurate linear registration and motion correction of brain images. NeuroImage 17 (2), 825–841. http://dx.doi.org/10.1006/nimg.2002.113212377157.
Jenkinson, M., Beckmann, C.F., Behrens, T.E., Woolrich, M.W., Smith, S.M., 2012. Fsl. NeuroImage 62 (2), 782–790. http://dx.doi.org/10.1016/j.neuroimage.2011.09.01521979382.
Kelly Jr., R.E., Alexopoulos, G.S., Wang, Z., Gunning, F.M., Murphy, C.F., Morimoto, S.S., Kanellopoulos, D., Jia, Z., Lim, K.O., Hoptman, M.J., 2010. Visual inspection of independent components: defining a procedure for artifact removal from fMRI data. J. Neurosci. Methods 189 (2), 233–245. http://dx.doi.org/10.1016/j.jneumeth.2010.03.02820381530.
Kish, S.J., Shannak, K., Hornykiewicz, O., 1988. Uneven pattern of dopamine loss in the striatum of patients with idiopathic Parkinson's disease. pathophysiologic and clinical implications. N. Engl. J. Med. 318 (14), 876–880. http://dx.doi.org/10.1056/NEJM198804073181402335267 2.
Krajcovicova, L., Mikl, M., Marecek, R., Rektorova, I., 2012. The default mode network integrity in patients with Parkinson's disease is levodopa equivalent dose-dependent. J. Neural Transm. 119 (4), 443–454. http://dx.doi.org/10.1007/s00702-011-0723-522002597.
Kwak, Y., Peltier, S., Bohnen, N.I., Müller, M.L., Dayalu, P., Seidler, R.D., 2010. Altered resting state cortico-striatal connectivity in mild to moderate stage Parkinson's disease. Front. Syst. Neurosci. 4, 143. http://dx.doi.org/10.3389/fnsys.2010.0014321206528.
Laird, A.R., Fox, P.M., Eickhoff, S.B., Turner, J.A., Ray, K.L., McKay, D.R., Glahn, D.C., Beckmann, C.F., Smith, S.M., Fox, P.T., 2011. Behavioral interpretations of intrinsic connectivity networks. J. Cogn. Neurosci. 23 (12), 4022–4037. http://dx.doi.org/10.1162/jocn_a_0007721671731.
Laird, A.R., Lancaster, J.L., Fox, P.T., 2005. BrainMap: the social evolution of a human brain mapping database. Neuroinformatics 3 (1), 65–78. http://dx.doi.org/10.1385/NI:3:1:06515897617.
Leh, S.E., Chakravarty, M.M., Ptito, A., 2008. The connectivity of the human pulvinar: a diffusion tensor imaging tractography study. Int. J. Biomed. Imaging 2008, 789539. http://dx.doi.org/10.1155/2008/78953918274667.
Lewis, S.J., Dove, A., Robbins, T.W., Barker, R.A., Owen, A.M., 2003. Cognitive impairments in early Parkinson's disease are accompanied by reductions in activity in frontostriatal neural circuitry. J. Neurosci. 23 (15), 6351–6356 12867520.
Lewis, S.J., Slabosz, A., Robbins, T.W., Barker, R.A., Owen, A.M., 2005. Dopaminergic basis for deficits in working memory but not attentional set-shifting in Parkinson's disease. Neuropsychologia 43 (6), 823–832. http://dx.doi.org/10.1016/j.neuropsychologia.2004.10.00115716155.
Lozza, C., Marié, R.M., Baron, J.C., 2002. The metabolic substrates of bradykinesia and tremor in uncomplicated Parkinson's disease. NeuroImage 17 (2), 688–699. http://dx.doi.org/10.1006/nimg.2002.124512377144.
Macdonald, P.A., Monchi, O., 2011. Differential effects of dopaminergic therapies on dorsal and ventral striatum in Parkinson's disease: implications for cognitive function. Parkinson's Dis. 2011, 1–18. http://dx.doi.org/10.4061/2011/572743.
McKeown, M.J., Hansen, L.K., Sejnowsk, T.J., 2003. Independent component analysis of functional MRI: what is signal and what is noise? Curr. Opin. Neurobiol. 13 (5), 620–629. http://dx.doi.org/10.1016/j.conb.2003.09.01214630228.
MDS, 2003. The Unified Parkinson's Disease Rating Scale (UPDRS): status and recommendations. Mov. Disord. 18 (7), 738–750. http://dx.doi.org/10.1002/mds.1047312815652.
Menon, V., 2011. Large-scale brain networks and psychopathology: a unifying triple network model. Trends Cogn. Sci. 15 (10), 483–506. http://dx.doi.org/10.1016/j.tics.2011.08.00321908230.
Menon, V., Uddin, L.Q., 2010. Saliency, switching, attention and control: a network model of insula function. Brain Struct. Funct. 214 (5–6), 655–667. http://dx.doi.org/10.1007/s00429-010-0262-020512370.
Monchi, O., Petrides, M., Mejia-Constain, B., Strafella, A.P., 2007. Cortical activity in Parkinson's disease during executive processing depends on striatal involvement. Brain 130 (1), 233–244. http://dx.doi.org/10.1093/brain/awl32617121746.
Ongür, D., Lundy, M., Greenhouse, I., Shinn, A.K., Menon, V., Cohen, B.M., Renshaw, P.F., 2010. Default mode network abnormalities in bipolar disorder and schizophrenia. Psychiatry Res. 183 (1), 59–68. http://dx.doi.org/10.1016/j.pscychresns.2010.04.00820553873.
Poletti, M., Bonuccelli, U., 2013. Acute and chronic cognitive effects of levodopa and dopamine agonists on patients with Parkinson's disease: a review. Ther. Adv. Psychopharmacol. 3 (2), 101–113. http://dx.doi.org/10.1177/2045125312470130241676 81.
Raichle, M.E., MacLeod, A.M., Snyder, A.Z., Powers, W.J., Gusnard, D.A., Shulman, G.L., 2001. A default mode of brain function. Proc. Natl. Acad. Sci. U. S. A. 98 (2), 676–682. http://dx.doi.org/10.1073/pnas.98.2.67611209064.
Raichle, M.E., Mintun, M.A., 2006. Brain work and brain imaging. Annu. Rev. Neurosci. 29, 449–476. http://dx.doi.org/10.1146/annurev.neuro.29.051605.11281916776593.
Ravina, B., Marek, K., Eberly, S., Oakes, D., Kurlan, R., Ascherio, A., Beal, F., Beck, J., Flagg, E., Galpern, W.R., Harman, J., Lang, A.E., Schwarzschild, M., Tanner, C., Shoulson, I., 2012. Dopamine transporter imaging is associated with long-term outcomes in Parkinson's disease. Mov. Disord. 27 (11), 1392–1397. http://dx.doi.org/10.1002/mds.2515722976926.
Schendan, H.E., Tinaz, S., Maher, S.M., Stern, C.E., 2013. Frontostriatal and mediotemporal lobe contributions to implicit higher-order spatial sequence learning declines in aging and Parkinson's disease. Behav. Neurosci. 127 (2), 204–221. http://dx.doi.org/10.1037/a003201223565935.
Seeley, W.W., Menon, V., Schatzberg, A.F., Keller, J., Glover, G.H., Kenna, H., Reiss, A.L., Greicius, M.D., 2007. Dissociable intrinsic connectivity networks for salience processing and executive control. J. Neurosci. 27 (9), 2349–2356. http://dx.doi.org/10.1523/JNEUROSCI.5587-06.200717329432.
Shine, J.M., Matar, E., Ward, P.B., Frank, M.J., Moustafa, A.A., Pearson, M., Naismith, S.L., Lewis, S.J., 2013. Freezing of gait in Parkinson's disease is associated with functional decoupling between the cognitive control network and the basal ganglia. Brain 136 (12), 3671–3681. http://dx.doi.org/10.1093/brain/awt27224142148.
Shulman, R.G., Rothman, D.L., Behar, K.L., Hyder, F., 2004. Energetic basis of brain activity: implications for neuroimaging. Trends Neurosci. 27 (8), 489–495. http://dx.doi.org/10.1016/j.tins.2004.06.00515271497.
Smith, S.M., 2002. Fast robust automated brain extraction. Hum. Brain Mapp. 17 (3), 143–155. http://dx.doi.org/10.1002/hbm.1006212391568.
Sridharan, D., Levitin, D.J., Menon, V., 2008. A critical role for the right fronto-insular cortex in switching between central-executive and default-mode networks. Proc. Natl. Acad. Sci. U S A 105 (34), 12569–12574. http://dx.doi.org/10.1073/pnas.0800005105185723676.
Supekar, K., Menon, V., Rubin, D., Musen, M., Greicius, M.D., 2008. Network analysis of intrinsic functional brain connectivity in Alzheimer's disease. PLOS Comput. Biol. 4 (6). http://dx.doi.org/10.1371/journal.pcbi.100010018584043.
Tessitore, A., Esposito, F., Vitale, C., Santangelo, G., Amboni, M., Russo, A., Corbo, D., Cirillo, G., Barone, P., Tedeschi, G., 2012. Default-mode network connectivity in cognitively unimpaired patients with Parkinson disease. Neurology 79 (23), 2226–2232. http://dx.doi.org/10.1212/WNL.0b013e31827689d623100395.
Tinaz, S., Schendan, H.E., Stern, C.E., 2008. Fronto-striatal deficit in Parkinson's disease during semantic event sequencing. Neurobiol. Aging 29 (3), 397–407. http://dx.doi.org/10.1016/j.neurobiolaging.2006.10.02517157417.
Tomlinson, C.L., Stowe, R., Patel, S., Rick, C., Gray, R., Clarke, C.E., 2010. Systematic review of levodopa dose equivalency reporting in Parkinson's disease. Mov. Disord. 25 (15), 2649–2653. http://dx.doi.org/10.1002/mds.2342921069833.
Van den Heuvel, M.P., Mandl, R.C., Kahn, R.S., Hulshoff Pol, H.E., 2009. Functionally linked resting-state networks reflect the underlying structural connectivity architecture of the human brain. Hum. Brain Mapp. 30 (10), 3127–3141. http://dx.doi.org/10.1002/hbm.2073719235882.
Van Eimeren, T., Monchi, O., Ballanger, B., Strafella, A.P., 2009. Dysfunction of the default mode network in Parkinson disease: a functional magnetic resonance imaging study. Arch. Neurol. 66 (7), 877–883. http://dx.doi.org/10.1001/archneurol.2009.9719597090.
Wang, D., Buckner, R.L., Liu, H., 2014. Functional specialization in the human brain estimated by intrinsic hemispheric interaction. J. Neurosci. 34 (37), 12341–12352. http://dx.doi.org/10.1523/JNEUROSCI.0787-14.201425209275.